Missouri University of Science and Technology
Scholars' Mine

International Specialty Conference on Cold-Formed Steel Structures

(1996) - 13th International Specialty Conference on Cold-Formed Steel Structures

Oct 17th, 12:00 AM

Evaluation and Modelling of the Material Properties for Analysis of Cold-formed Steel Sections

Nabil Abdel-Rahman

K. S. Sivakumaran

Follow this and additional works at: https://scholarsmine.mst.edu/isccss

 Part of the Structural Engineering Commons

Recommended Citation

Abdel-Rahman, Nabil and Sivakumaran, K. S., "Evaluation and Modelling of the Material Properties for Analysis of Cold-formed Steel Sections" (1996). *International Specialty Conference on Cold-Formed Steel Structures*. 3.
https://scholarsmine.mst.edu/isccss/13iccfss/13iccfss-session11/3

This Article - Conference proceedings is brought to you for free and open access by Scholars' Mine. It has been accepted for inclusion in International Specialty Conference on Cold-Formed Steel Structures by an authorized administrator of Scholars' Mine. This work is protected by U. S. Copyright Law. Unauthorized use including reproduction for redistribution requires the permission of the copyright holder. For more information, please contact scholarsmine@mst.edu.

Thirteenth International Specialty Conference on Cold-Formed Steel Structures
St. Louis, Missouri U.S.A., October 17-18, 1996

EVALUATION AND MODELLING OF THE MATERIAL PROPERTIES FOR ANALYSIS OF COLD-FORMED STEEL SECTIONS

Nabil Abdel-Rahman[1] and K. S. Sivakumaran[2]

Abstract

The results of two series of experimental investigations to evaluate the mechanical properties and the residual stresses of cold-formed steel (CFS) sections are reported in this paper. These investigations were performed on channel-shaped CFS sections manufactured using cold-roll forming technique. Tensile coupon tests were used to evaluate the mechanical properties at different positions of the channel sections. Electrical resistance strain gauges with an "Electrical Discharge Machining" cutting technique were used to establish the magnitudes and the distributions of residual stresses within the channel sections. Based on the experimental results, appropriate analysis models for the stress-strain relationship, the variation of the yield strength, and the residual stresses in CFS channel sections are established. These models are incorporated within a large deformation shell finite element to form a model for cold-formed steel sections. The finite element model is evaluated against experimental results of CFSsections in compression.

1. Introduction

The development of an appropriate analytical model to predict the behaviour of cold-formed steel (CFS) structural members requires a correct representation of the corresponding material characteristics. The steel characteristics that are of interest include (a) mechanical properties (uniaxial stress-strain behaviour, including values for the proportional limit, the yield and ultimate strengths, the yielding plateau, and strain hardening) and (b) residual stress state (initial pre-loading state of stress). The techniques used in the manufacture of CFS sections, such as cold-roll forming, are expected to induce substantial changes on the characteristics of the CFS material, as compared to virgin sheet steel. Large deformations are expected to occur in the section due to the cold bending operation. The deformations expected at flat parts of the section may be elastic deformations, however, the deformations expected at corner parts of the section are essentially plastic deformations. Once the cold bending operation is completed and the formed section is released, the elastic deformations at flat parts and the released elastic strains at corner parts can not recover due to the shape restriction. This behaviour results in the generation of trapped longitudinal and transversal residual stresses in the section. Meanwhile, the unreleased plastic strains at corner parts result in significant changes in the mechanical properties of the material due to "strain aging" phenomenon (Chajes et al., 1963).

1. Graduate Student, 2. Associate Professor,
Department of Civil Engineering, McMaster University, Hamilton, Ontario, CANADA. L8S 4L7

In general, the non-uniformity of the cold work applied to a CFS section results in different mechanical properties and different magnitudes of residual stresses across the section. Limited experimental studies on the effects of the cold work on the mechanical properties of CFS sections (Karren and Winter, 1967 and Coetsee, et al., 1990) and on the generation of residual stresses (Ingvarsson, 1977 and Weng and Pekoz, 1990) have been reported in the literature. This may be due to the well-known design idea that the existence of residual stresses in CFS sections cancels the effects of any improvement in the material properties due to strain hardening and aging.

This paper presents the results of two series of experimental investigations to evaluate the mechanical properties and the residual stresses of CFS sections. The investigations were performed on zinc-coated lipped channel sections manufactured in Canada using the method of cold-roll forming. Two different sections of steel type A 446/A 446M (ASTM, 1994) were considered in the study. The first section was a 203 mm (8 in.) deep, 1.91 mm (0.075 in.-14 gauge) thick, Grade D steel with a minimum specified yield strength of 345 MPa (50 ksi). The second section was a 101.5 mm (4 in.) deep, 1.22 mm (0.048 in.-18 gauge) thick, Grade A steel with a minimum specified yield strength of 228 MPa (33 ksi). Based on the current results and the results of previous researchers, this paper proposes analysis models for the variation of the yield strength, the stress-strain relationship, and the distribution of residual stresses across CFS channel sections. The paper also compares the results of a finite element analysis using the proposed models to the experimental results of CFS sections subjected to axial compressive loads.

2. Mechanical Properties of Cold-Formed Steel Sections

The mechanical properties of the cold-formed steel (CFS) channel sections were evaluated based on 41 tensile coupon tests. The coupons were cut along the longitudinal direction of the two channel sections. The exact positions of the coupons in the web, flanges, corners, and lips of the sections are shown in Figure 1(a). For each position, a minimum of two coupons were tested.

2.1 Preparation of Tensile Coupons and Test Procedure

The tensile coupons consisted of (a) 13 standard flat coupons (positions A-4, A-8, A-9, B-4, and B-8, length 200 mm, width 12.50 mm), (b) 19 non-standard flat coupons (positions A-1, A-3, A-5, A-7, B-1, B-3, B-5, and B-7, length 200 mm, width 6.25 mm), and (c) 9 non-standard curved coupons (positions A-2, A-6, B-2, and B-6, length 300 mm, corner width). The standard flat coupons were dimensioned according to the guidelines provided by the ASTM Standards A370-92, "Standard Test Methods and Definitions for Mechanical Testing of Steel Products", (ASTM, 1994) for sheet-type materials. The non-standard flat coupons had narrower width to be close to the corners. The curved coupons were dimensioned longer than the flat coupons to minimize the bending effects in the centre of the specimen during testing. The grip sections of the curved coupons were not flattened so that to keep the centre of the applied tensile force during the test aligned with the centre of the specimen within the gage length.

The tensile coupons were tested in a 250-kN capacity MTS (Material Test System) machine. A load range of 10% (with a full load of 25 kN) was adopted for the test. The coupons were mounted in the testing machine using the gripping devices and aligned with the vertical axis of the machine. The axial load was applied at a constant rate of 3.0 mm/min. A calibrated

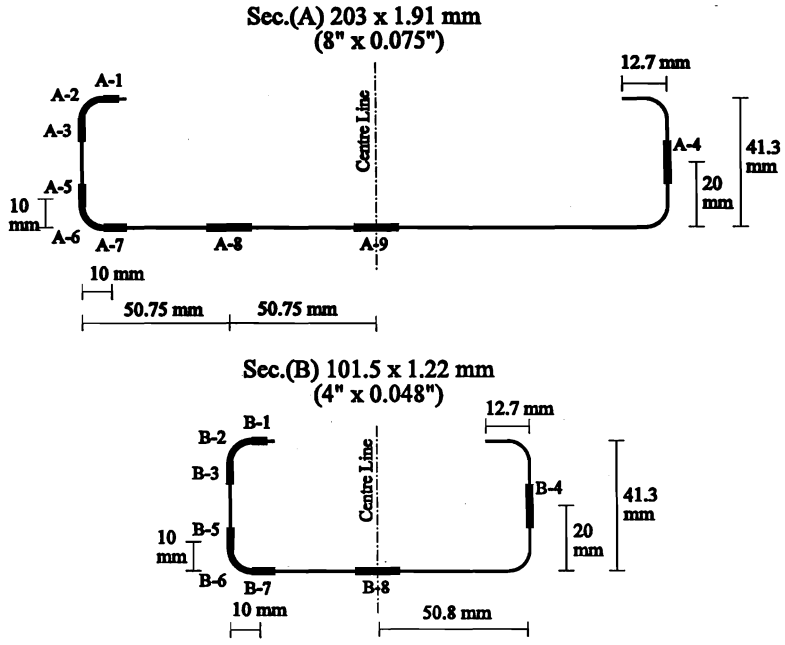

Figure 1(a) Positions of tensile coupons for sections (A) and (B)

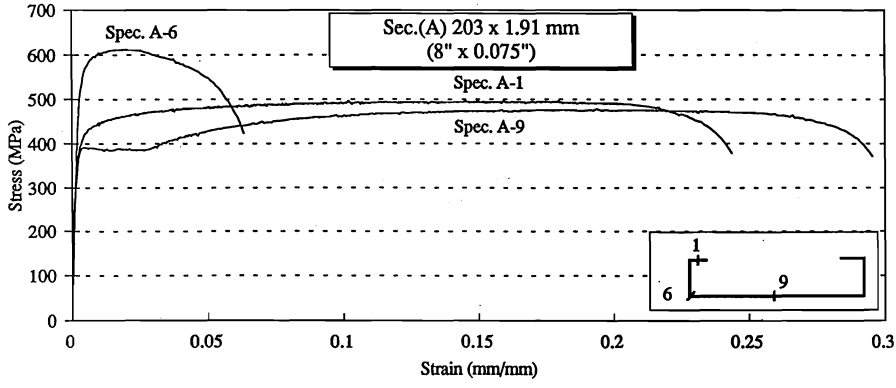

Figure 1(b) Stress-strain curves for cold-formed steel channel section (A)

extensometer of 50 mm gage length was used to measure the axial elongation of the coupons during the test. A strain range of 10% was adopted for the initial part of the test in order to increase the accuracy of the elongation readings during the elastic behaviour of the coupons. The strain range was then increased to 50%, beyond an equivalent strain limit of 0.02, in order to monitor the plastic behaviour of the coupons up to failure. The voltage readings of both the axial load and the axial elongation during the test were recorded using a two-channel data acquisition system. A real time display of the load-elongation relationship during the test was obtained by connecting a personal computer with a "Lab-Tech Notebook" computer software to the data acquisition system.

2.2 Tensile coupon Test Results

The stress-strain relationship of a tensile coupon was derived from the load-elongation relationship using its original cross-sectional area and the gage length. The cross-sectional area of a flat coupon was determined by measuring the actual minimum width and thickness within the gage length to the nearest 0.01 mm. The minimum base thickness was determined by excluding the coating thickness. The cross-sectional area of a curved coupon was determined from the geometry of the corner part of the section, knowing the base thickness and the inside and outside radii. Figure 1(b) shows a sample of the resulting stress-strain curves for section (A). In this figure, note that the specimens A-1, A-6, and A-9 were taken at the lip, rounded corner, and at the web, respectively. Similar curves were derived for all tensile coupons, but are not shown here due to the space limit. However, the average results of the mechanical properties, calculated from such experimental stress-strain curves, for the two test sections have been presented in Table 1.

The results show that tensile coupons from flat parts have approximately the same stress-strain relationship, yield strength, ultimate strength, and elongation. Although actual data about the properties of the virgin steel sheet is not available, this behaviour of the flat parts suggests that the cold-roll forming operation did not affect the flat parts of the section. However, the substantial changes in the material behaviour are noticed at and around the corner parts as a result of the large plastic deformations of the cold forming operation. A considerable increase in the yield and ultimate strengths (of at least 23% and up to 47%, depending on the steel grade) occur at the corner parts of both the test sections (A) and (B). This increase is accompanied by a severe decrease in ductility and a disappearance of the yielding plateau and the strain hardening range. The changes adjacent to the corner parts (represented by the next-to-corner coupons) are not as significant as for the corner parts, but generally higher than flat parts.

The steel grade of the test sections is found to have an effect on the yielding type of the tensile coupons. As indicated in Table 1, while all the coupons of the test section (A) (Grade D steel) experienced a gradual yielding type, only the corner coupons of the test section (B) (Grade A steel) experienced the gradual yielding type. The other coupons of section (B) showed either a sharp yielding or a non-defined (mixed) yielding type.

Table 1 Average mechanical properties of tensile coupons for sections (A) and (B)

Position	A-1	A-2	A-3	A-4	A-5	A-6	A-7	A-8	A-9	B-1	B-2	B-3	B-4	B-5	B-6	B-7	B-8
Pos. Type	Lip	Corner	Next to corner	Flat	Next to corner	Corner	Next to corner	Flat	Flat	Lip	Corner	Next to corner	Flat	Next to corner	Corner	Next to corner	Flat
E (GPa)	196.7	194.9	193.7	195.2	188.2	214.1	191.8	195.2	195.2	184.6	185.8	197.3	183.7	192.7	210.4	189.6	187.8
F_p (MPa)[a]	277.8	362.5	290.6	292.8	286.8	383.3	286.0	292.8	292.8	--	352.4	--	--	--	342.5	--	--
F_y (MPa)[b]	405.1	552.3	397.9	385.2	397.1	565.0	379.4	385.2	385.2	357.2	400.1	333.9	320.0	328.3	392.0	335.7	318.1
Yielding Type[c]	G	G	G	G	G	G	G	G	G	S	G	N	N	S	G	S	N
F_u (MPa)	495.3	604.9	481.8	475.0	477.2	614.8	479.3	475.0	475.0	410.0	453.3	364.5	362.0	362.3	450.2	371.7	362.0
Elong. %	25.9	8.2	25.0	30.1	26.0	6.5	28.1	30.1	32.2	21.9	12.1	33.2	35.8	32.0	12.3	30.0	36.1
F_p / F_y	0.69	0.66	0.73	0.76	0.72	0.68	0.75	0.76	0.76	--	0.88	--	--	--	0.87	--	--
F_u / F_y	1.22	1.10	1.21	1.23	1.20	1.09	1.26	1.23	1.23	1.15	1.13	1.09	1.13	1.10	1.15	1.11	1.14
$F_y / F_{y\,flat}$	1.05	1.43	1.03	1.0	1.03	1.47	0.98	1.0	1.0	1.12	1.26	1.05	1.0	1.03	1.23	1.06	1.0
$F_u / F_{u\,flat}$	1.04	1.27	1.02	1.0	1.01	1.29	1.01	1.0	1.0	1.13	1.25	1.01	1.0	1.0	1.24	1.03	1.0

[a] F_p is the 0.01% offset strength for gradual yielding materials
[b] F_y is the 0.2% offset strength for gradual yielding materials and the yield stress for sharp yielding materials
[c] S represents sharp yielding, G represents gradual yielding, and N represents non-defined shape of yielding

2.3 Model for Variation of Yield Strength

The current tensile coupon test results, as well as the results given by Karren and Winter (1967) and Coetsee et al. (1990), show a significant increase in the yield strength in cold-formed steel (CFS) channel sections, particularly at the corner areas and flat areas adjacent to corners. To incorporate the variation of the yield strength into an analytical model of the CFS material, it is proposed that a lipped channel CFS section be divided into two zones; a corner zone and a flat zone. Figure 2(a) identifies the suggested corner zone and the flat zone of a lipped channel section. The corner zone includes all the four curved areas of the section, two equivalent flat areas on both sides of each curved area, and the two lips of the section. The flat zone includes the rest of the flat area of the web and flanges of the section. Each zone will be assigned appropriate but different mechanical properties.

Based on the results of the tensile coupons, the yield strength of the flat zone (F_y) is proposed to be uniform, and represented by the value of the minimum specified yield strength of the steel grade of the section. This means that no increase in the yield strength is to be considered in the flat zone of the section. The yield strength of the corner zone (F_{yc}) is proposed to have higher value than the corresponding strength of the flat zone.

Karren (1967) developed a semi-analytical model to predict the increase in the corner yield strength (ΔF_y) as follows:

$$\Delta F_y \ (\underline{\text{corner area}}) = \left[\frac{B_c}{(r/t)^m} - 1.0\right] F_y \qquad [1]$$

where,

$$B_c = 3.69 \left(\frac{F_u}{F_y}\right) - 0.819 \left(\frac{F_u}{F_y}\right)^2 - 1.79 , \quad m = 0.192 \left(\frac{F_u}{F_y}\right) - 0.068$$

This model suggests that the increase in yield strength at corners is dependant on the ratio between the ultimate strength (F_u) and yield strength (F_y) of the virgin steel material, the inside bending radius of the corner (r), and the thickness of the flat steel sheet (t). The model can be used to predict the increase in the yield strength of the corner area only and is not valid for areas adjacent to corners (which show increased yield strengths as well). Therefore, the current test results and the results given by Karren and Winter (1967), for different shapes of rolled CFS sections,were compared to Equation (1). It was observed that the average increase in the yield strengths measured within the corner zone, as compared to the flat zone yield strength (F_y), usually ranges between 0.60 and 0.69 of the values predicted by Equation (1). Hence, it is proposed to use Karren's model to predict the yield strength of the corner zone (F_{yc}), however a factor is added to Equation (1) as follows:

$$\Delta F_y \ (\underline{\text{corner zone}}) = 0.65 \left[\frac{B_c}{(r/t)^m} - 1.0\right] F_y \qquad [2]$$

Figures 2(b) and (c) show the proposed model for the distribution of the yield strength across the lipped channel section and the measured distribution given by the tensile coupon tests for both sections (A) and (B).

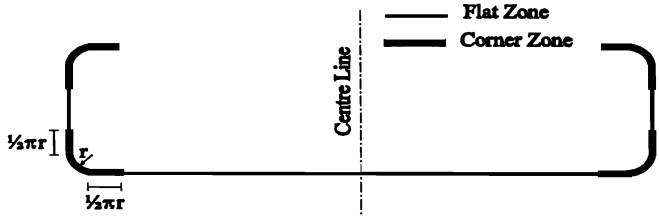

Figure 2(a) Definition of flat and corner zones of a lipped channel section

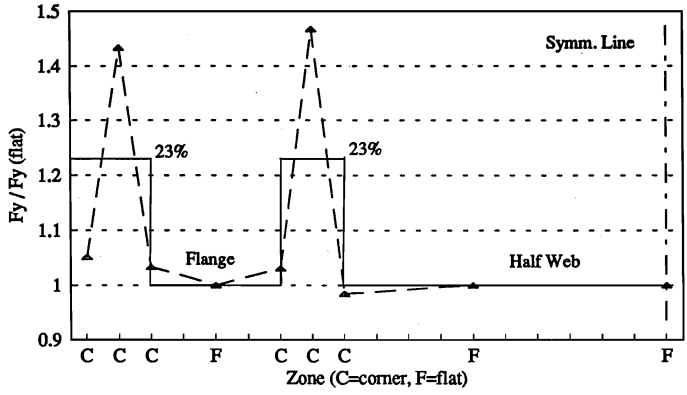

(b) Sec. (A) - Grade D Steel

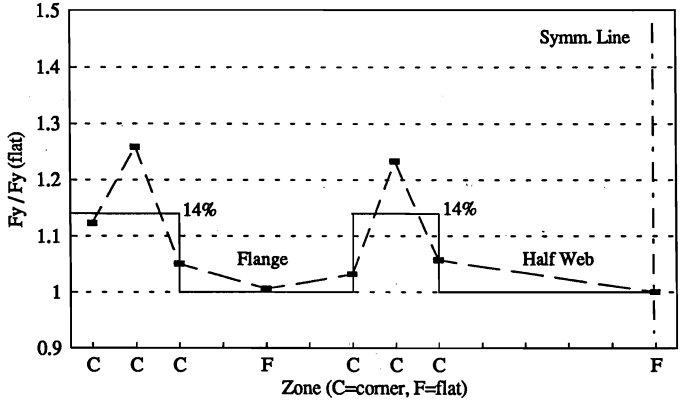

(c) Sec. (B) - Grade A Steel

Figure 2(b),(c) Measured and idealized yield strength for channel sections of Grades D and A steels

2.4 Model for Stress-Strain Relationship

As a gradual yielding behaviour was observed in most of the tensile coupons, an idealized elasto-plastic stress-strain model with a multi-linear isotropic strain hardening rule may be used to account for this behaviour. The proposed idealized model, as shown in Figure 3, is based on the Huber-von Mises elasto-plastic stress-strain model (Chen and Han, 1988).

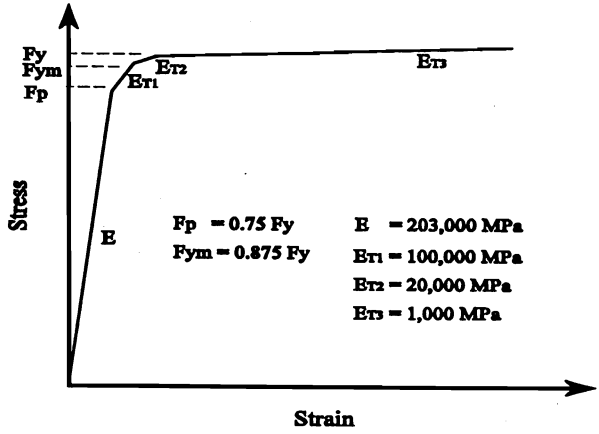

Figure 3 Idealized stress-strain relationship for cold-formed steel

In this idealized model, the elastic stress-strain behaviour is represented by a linear segment with a slope equals to the modulus of elasticity (E) up to a proportional strength limit (F_p), which is equivalent to the initial yielding point of the material. The gradual yielding behaviour can be idealized using a bi-linear representation (with tangent moduli E_{T1} and E_{T2}) between the proportional limit (F_p) and the yield strength (F_y) passing through an intermediate yielding strength (F_{ym}). This intermediate strength (F_{ym}) is taken as the half-way point strength between (F_p) and (F_y). The strain hardening behaviour is next represented by a linear segment with a tangent moduli (E_{T3}). The limit strengths of the idealized stress-strain relationship (F_p, F_{ym}, and F_y) for the corner zone and the flat zone of the channel section follow the idealization of the yield strength presented in section 2.3. A ratio of (F_p/ F_y) equals to 0.75 is considered appropriate (based on the test results) for both the flat zone and the corner zone of the section. The modulus of elasticity (E) is considered equal to 203,000 MPa (CSA, 1994 and AISI, 1991). The proposed values for the tangent moduli (E_{T1}, E_{T2}, and E_{T3}) are 100,000 MPa, 20,000 MPa, and 1,000 MPa, respectively, which are the best approximation of the results of the tensile coupons.

3. Residual Stresses in Cold-Formed Steel Sections

The magnitudes and distributions of longitudinal and transversal residual surface strains at different positions of cold-formed steel (CFS) channel sections were investigated in this part of the study. The surface strains were released by slicing the sections into strips using the method of Electrical Discharge Machining (EDM), and the strains were measured using electrical resistance strain gauges.

3.1 Electrical Discharge Machining Method

Electrical Discharge machining (EDM) is a non-traditional machining process of metals using sparks (electrical discharges). The sparks occur in the gap between the cutting tool (electrode) and the test specimen (workpiece) in an environment of ionized dielectric fluid (Weller and Haavisto, 1984). The use of the EDM method for a residual stress test is considered a relatively new technique as most of the work done before, except for the study by Weng and Pekoz (1990), was based on conventional saw cutting. The advantages of using the EDM method over the saw method are; (a) Avoiding permanent deformations of the test section as excessive clamping is not needed, (b) Avoiding vibrations during the cutting process as there is no contact between the cutting tool and the test specimen, and (c) The dielectric fluid works as a coolant and also as an insulator between the tool and the specimen. The EDM machine used in the investigation was a knee-type, quill-head TQH-31 compact electrical discharge machine. The cutting tool was made of brass, as it is an excellent conduction material, and was shaped as a rectangular plate having a thickness of 1 mm. Since the brass cutting tool erodes during the cutting process, a new tool had to be used after every 3 or 4 cuts. A hydrocarbon oil was used as a dielectric fluid and was continuously circulated during the cutting process to flush away the removed material particles.

3.2 Preparation of Specimens and Test Procedure

Residual stress tests were performed on two identical specimens for each of section (A) and section (B). The test specimens were saw-cut from long CFS columns, well away from the ends to avoid any end damage of the columns. The length of the specimens of section (A) was 600 mm, and of section (B) was 300 mm. The specimens were prepared for mounting the strain gauges by removing the zinc coating layer at the positions of the gauges using a 50% solution of the hydrochloric acid. Fourteen strain gauges were mounted on each test specimen of section (A) and 12 strain gauges were mounted on each test specimen of section (B). The positions of the strain gauges on the specimens of sections (A) are shown in Figure 4(a). As shown in the figure, the strain gauges were mounted on both the inside and outside surfaces of the specimens at each position, except at the lip and the adjacent corner where no gauges were mounted on the inside surface as it was difficult to reach. All the strain gauges were of 5 mm length and were mounted in the longitudinal direction of the section at the mid-length of the test specimen. One 5 mm rosette strain gauge was also mounted at position (8) of the second test specimen of section (A) to measure the surface strains in the longitudinal, transversal, and 45 degrees directions of the specimen. The strain data was recorded by connecting the strain gauges of a single test specimen to a strain indicator (Model P-3500) through switch and balance units (Model SB-1).

The specimen, along with the attached strain gauges, was placed inside the workpan of the TQH-31 machine and lightly clamped to the bed of the pan at its edges. The workpan was then filled with the hydrocarbon oil and the brass cutting tool was mounted in its place. Reading of each strain gauge was initialized to zero using the switch and balance units. The cutting sequence for the test specimens of section (A) around the strain gauges is shown in Figure 4(b). The specimen was supported underneath each cutting path to prevent any local deformations in the surrounding area of the cut. When the whole cutting sequence was completed, the cut strips were taken out of the workpan, and were left for about 3 minutes to cool down to the normal room temperature. The readings of all the strain gauges were then recorded using the strain indicator.

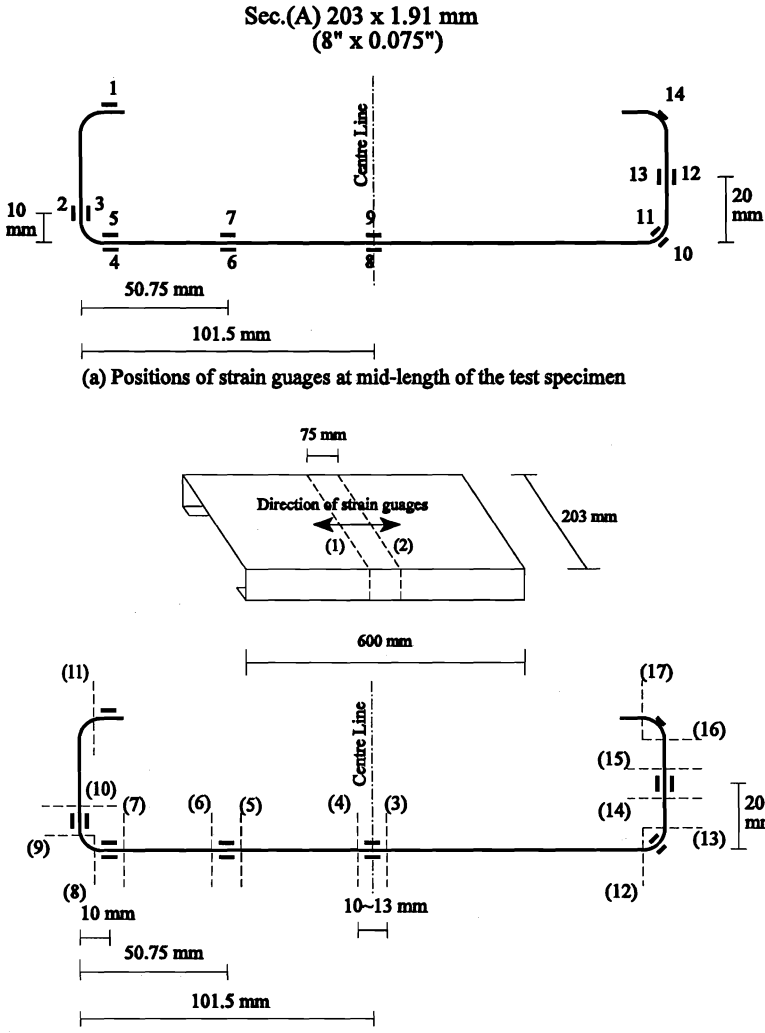

Figure 4 Positions of strain gauges for residual strains and cutting sequence for section (A)

3.3 Residual Stress Test Results

The measured values of the released surface strains for section (A) and section (B) are given in Table 2, in which a negative surface strain corresponds to a tensile (positive) residual surface stress, and a positive surface strain corresponds to a compression (negative) residual surface stress. The unreported data at gauges (1) and (14) indicate inside surface locations where strain gauges could not be attached. The measured surface strains of CFS channel sections indicate that significant surface residual stresses exist in these sections due to the cold roll-forming operation. Tensile residual stresses were recorded on the outside surface of the channel sections, and compression residual stresses were recorded on the inside surface of the channel sections. This observation was consistent with all the test specimens of sections (A) and (B). The major effect of the forming operation, at the location of the highest magnitudes of residual stresses, is found at the web area next to the curved corner (gauges 4 and 5) for all the test specimens. The lip area (gauge 1) and the flange-lip corner (gauge 14) also show relatively high magnitudes of residual stresses. The web-flange corner (gauges 10 and 11) shows lower magnitudes of residual stresses compared to the flange-lip corner. This behaviour may be attributed to the forming technique and the arrangement of forming rolls. Unfortunately, information about the actual forming technique and the arrangement of rolls used by the manufacturer are not available.

An important observation from the test results reported in Table 2 is that the magnitude of the residual stresses on the outside surface of a section at every location is very close to the corresponding magnitude of the residual stresses on the inside surface, however, with an opposite sign. Similar observations were reported in the theoretical study carried out by Ingvarsson (1977) and the tests performed by Weng and Pekoz (1990). This observation may be interpreted as that the residual stress distribution in a thin section changes from tensile to compression through the thickness, with a linear shape and having almost a zero stress at the centre line of the section. The residual stresses in both the longitudinal and transversal directions were investigated at one location on the web plate of section (A). The first and second principal strains at this location were found to be (-286.5 $\mu\varepsilon$) and (+13.5 $\mu\varepsilon$), respectively. It can be noticed that the difference between the first principal strain and the recorded longitudinal strain (-284 $\mu\varepsilon$) at that location is less than 1%. This suggests that the longitudinal direction of a CFS section is the principal residual stress direction. It also indicates that the magnitudes of transversal residual strains for structural CFS sections are not significant compared to the longitudinal residual strains.

3.4 Model for Residual Stress Distribution

Based on the current results and the results given by Weng and Pekoz (1990), it is proposed that the residual stress distributions for sections (A) and (B) be modelled as shown in Figures 5(a) and (b). It is found that a ratio between the longitudinal residual stress and the yield strength (F_{rl} / F_y) equals to 40% for the corner zone (as defined in section 2.3) represents the average of the measured residual stresses in this zone for all the test specimens in the current study. This ratio is less than the ratio of 50% suggested by Weng and Pekoz (1990). For the flat zone, an average ratio (F_{rl} / F_y) equals to 12% is found to represent the flat areas of section (A) and an average ratio (F_{rl} / F_y) equals to 18% is found to represent the flat areas of section (B). These ratios indicate that the cold work, and consequently the residual stresses, tend to increase on the web area when the web is short. Hence, it is suggested that the ratio (F_{rl} / F_y) in the flat zone of a

Table 2 Measured released surface strains for sections (A) and (B)

Section (A) Measuring gauges[a]	Surface strain (με) (ϵ_y = 1898 με)							
	Outside surface				Inside surface			
	Specimen (1)		Specimen (2)		Specimen (1)		Specimen (2)	
	ϵ	ϵ/ϵ_y	ϵ	ϵ/ϵ_y	ϵ	ϵ/ϵ_y	ϵ	ϵ/ϵ_y
1	-857	-0.452	-892	-0.470	--	--	--	--
14	-1188	-0.626	-1252	-0.660	--	--	--	--
12 , 13	-243	-0.128	-250	-0.132	+44	0.023	+75	0.040
2 , 3	-141	-0.074	-324	-0.171	+84	0.044	+111	0.058
10 , 11	-129	-0.068	-84	-0.044	+200	0.105	+126	0.066
4 , 5	-1366	-0.720	-1219	-0.642	+1272	0.670	+1342	0.707
6 , 7	-257	-0.135	-302	-0.159	+150	0.079	+220	0.116
8 , 9	-404	-0.213	-284	-0.150	+246	0.130	+180	0.095
			+11 (trans.)					
			-164 (45°)					

Section (B) Measuring gauges[a]	Surface strain (με) (ϵ_y = 1567 με)							
	Outside surface				Inside surface			
	Specimen (1)		Specimen (2)		Specimen (1)		Specimen (2)	
	ϵ	ϵ/ϵ_y	ϵ	ϵ/ϵ_y	ϵ	ϵ/ϵ_y	ϵ	ϵ/ϵ_y
1	-474	-0.302	-356	-0.227	--	--	--	--
14	N/A[b]	N/A	-388	-0.248	--	--	--	--
12 , 13	-149	-0.095	-152	-0.097	+79	0.050	+117	0.075
2 , 3	-157	-0.100	-171	-0.109	+221	0.141	+82	0.052
10 , 11	-236	-0.151	-252	-0.161	+258	0.165	N/A	N/A
4 , 5	-698	-0.445	-614	-0.392	+568	0.362	+609	0.389
8 , 9	N/A	N/A	-462	-0.295	N/A	N/A	+401	0.256

[a] Refer to Figure 4(a)
[b] Defective strain gauge during the cutting process

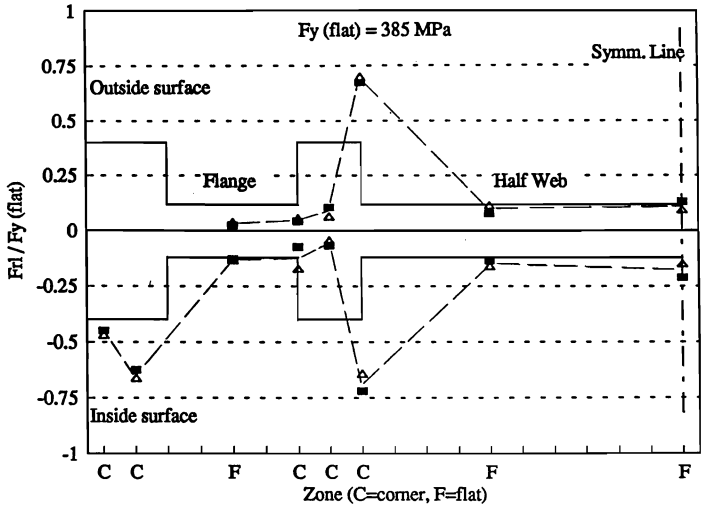

(a) Sec. (A) - Grade D Steel

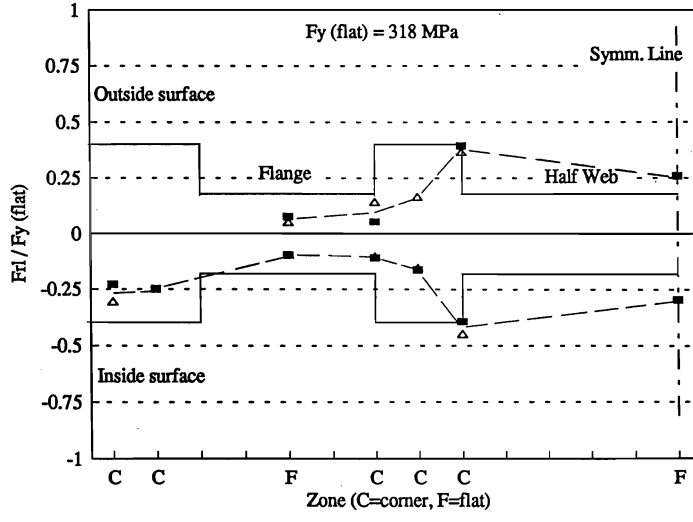

(b) Sec. (B) - Grade A Steel

Figure 5 Measured and idealized residual stresses for channel sections of Grades D and A steels

roll-formed channel section with any width can be assumed with the guide of the above given two ratios.

The residual stress distribution through the thickness can generally be considered linear across the whole section, with tensile stress on the outside surface and equal compression stress on the inside surface at the same location. The residual stress at any layer through the thickness can then be obtained from this linear distribution.

4. Application of Proposed Material Models in Analysis

The proposed models for the variation of the yield strength, the stress-strain relationship, and the residual stress distribution in cold-formed steel (CFS) sections were incorporated within a large deformation finite element computer model for analysis of CFS members (Abdel-Rahman and Sivakumaran, 1995). The finite element model utilizes a degenerated isoparametric shell finite element based on the method of "assumed transverse shear and membrane strain fields".

4.1 Test and Analysis of Cold-Formed Steel Members in Compression

To identify the efficiency of the proposed material models when applied for CFS members in compression, two similar stub-columns of section (A), having length equals to 475 mm, were tested up to failure under concentric axial loading. The stub-columns lengths were chosen such that to study the pre- and post-local buckling behaviour and to exclude the effects of overall buckling. The axial shortening of the two stub-columns and the strain distribution across the second stub-column were recorded during the tests along with the axial load. The test setup and procedure are explained in detail by Abdel-Rahman (1996).

A model for the stub-columns was prepared using the large deformation shell element. Figure 6(a) shows the finite element mesh for one quarter of the lipped channel stub-column. Symmetric boundary conditions were imposed at the symmetry lines of the one quarter of the stub-column. At the loading edge, the stub-column was subjected to a uniform displacement condition, rather than a uniform loading condition. The uniform displacement condition is achieved by applying an incremental compressive loading through rigid plate elements. This would mean then, the distribution of loading over the edges of the CFS member itself is not necessarily uniform and can take any shape depending on the level of loading. The rigid plate elements are restricted to undergo axial longitudinal displacements only. Fixed end conditions are imposed at the loaded edges of the CFS member to simulate the test. In order to determine the precise ultimate load, and the post-ultimate behaviour of the CFS members in compression, a displacement control algorithm was included within the general finite element program. Such an algorithm is based on a unified constraint procedure, which enables different control methods to be implemented according to the definition of the control parameters (Kanok-Nukulchai, 1990). The displacement control algorithm allows the displacement to be incremented at one control node within the finite element mesh. The solution of the governing equilibrium equations results in the load intensity at load/support points and the displacement vector at other points. The displacement algorithm was incorporated with the above mentioned uniform displacement loading technique by selecting a control node at the edge of the CFS member. In that case, the rigid plate elements maintain all the edge nodes of the member at the same displacement value of the incremented displacement.

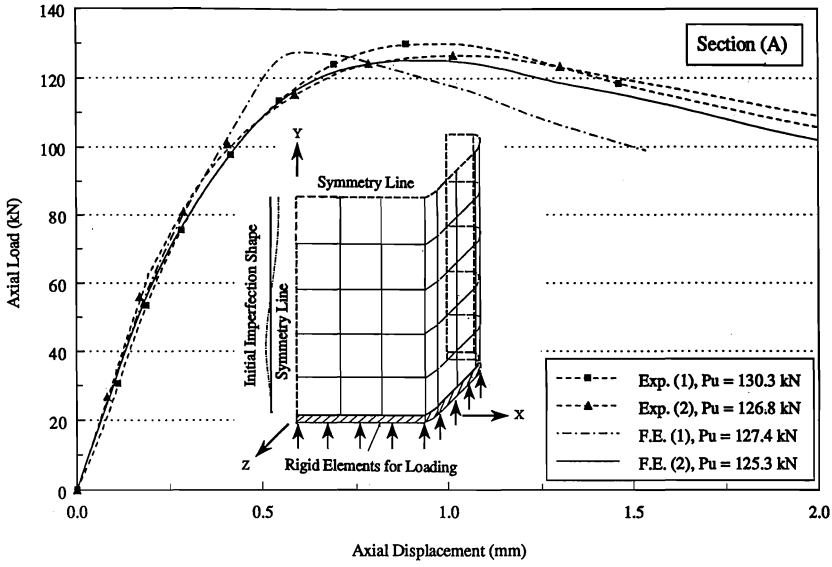

Figure 6(a) Axial load-axial displacement curves of the stub-column

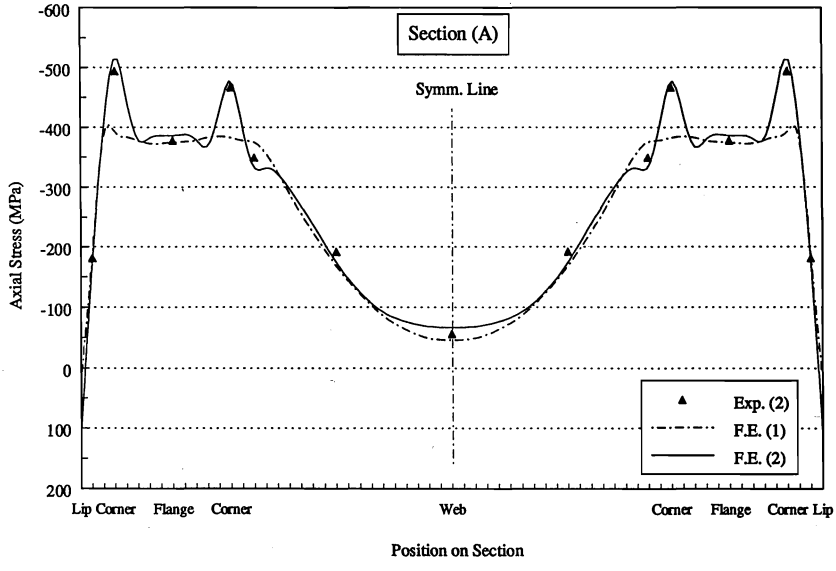

Figure 6(b) Axial stress distributions corresponding to ultimate load levels

Initial geometric imperfections were imposed on the finite element model as a double sine wave distribution in the web plate, with a half-wave length equals to the web plate width. This distribution is, in fact, the expected local buckling shape of the web plate.

4.2 Comparison of Results

Figure 6(a) shows the axial load-axial displacement curves obtained from the two stub-column tests (Exp. (1) and Exp. (2)), and from two finite element models (F.E. (1) and F.E. (2)). The first finite element model (F.E. (1)) does not consider any residual stresses, and considers an elastic-perfectly plastic stress-strain relationship with a yield strength equals to the flat yield strength value (385.2 MPa) across the whole section. The second finite element model (F.E. (2)) considers the material models proposed in the current study. The resulting ultimate load from each test and finite element model is also shown in the same figure. The results show that both finite element models are very efficient in predicting the deformations of the CFS section prior to yielding. Both models also predicted somewhat similar ultimate loads, which are in good agreement with the experimental ultimate loads. However, a significant difference is noticed between the behaviour of the two models when the section begins to yield. Model (F.E. (1)) could not show the gradual yielding of the section, and exhibited about 60% of the expected experimental axial displacement at the ultimate load level. Model (F.E. (2)) showed a gradual yielding behaviour, and post-ultimate behaviour, which are in excellent agreement with the experimental results. Figure 6(b) shows the axial stress distributions, corresponding to the ultimate load levels, of the second stub-column and the two finite element models. These stress distributions were recorded at the mid-height positions for both the test and the models. The figure shows that the model (F.E. (2)) well predicted the axial stress values across the section, specially at the corners and in the buckled web area. Model (F.E. (1)) could not predict the stress peaks at the corner since the increase in the yield strength at the corners was neglected.

The above comparisons indicate that the material models proposed herein are valuable in obtaining the true deformation behaviour and also the true stress distribution across CFS sections. It is very important to accurately establish the stress distribution at ultimate loads, since it is the basis for the "effective width" design concept used in codes (CSA, 1994 and AISI, 1991). The idea that the existence of residual stresses in CFS sections cancels the effects of increased yield strength might be acceptable when considering ultimate load value only, but it may not be valid when considering the deformation behaviour and stress distribution across the section.

5. Conclusions

The results of 41 tensile coupon tests to evaluate the mechanical properties of cold-formed steel (CFS) channel sections have been presented. Also the results of four residual stress tests to establish the magnitudes and distributions of residual stresses within the channel sections have been presented. Both series of tests showed that the cold bending operation alters the virgin material properties of the steel sheet, with the major changes at and around the corners of the sections. Models for the distribution of yield strength and residual stresses across channel sections have been presented and discussed. The models were used within a finite element computer model of sections in compression, and the results showed that the proposed models can effectively help in obtaining the true deformations and stress distribution across CFS sections.

Appendix: References

Abdel-Rahman, N. (1996), Analysis of Cold-Formed Steel Compression Members with Perforations, Ph.D. Thesis (in preparation), McMaster University, Hamilton, Ontario, Canada.

Abdel-Rahman, N. and Sivakumaran, K. S. (1995), Nonlinear Analysis of Cold-Formed Steel Members using Assumed Strain Shell Finite Elements, Proceedings of the Annual Conference of the Canadian Society for Civil Engineering, CSCE, Vol. IV, Ottawa, Ontario, Canada.

AISI (1991), Load and Resistance Factor Design Specification for Cold Formed Steel Structural Members, American Iron and Steel Institute, Washington, D.C., U.S.A.

ASTM Standards (1994). Iron and Steel Products - Coated Steel Products, American Society for Testing and Materials, Vol. 1.6, Designation A 446/A 446M, Philadelphia, U.S.A.

Chajes, A., Britvec, S. J., and Winter, G. (1963), Effects of Cold Straining on Structural Sheet Steels, Journal of the Structural Division, ASCE, Vol. 89, No. ST4, pp. 1-32.

Chen, W. F. and Han, D. J. (1988), Plasticity for Structural Engineers, Springer-Verlag Inc., New York, U.S.A.

Coetsee, J. S., Van den Berg, G. J., and Van der Merwe, P. (1990), The Effect of Workhardening and Residual Stresses due to Cold Working of Forming on the Strength of Cold-Formed Stainless Steel Lipped Channel Sections, 10th International Specialty Conference on Cold-Formed Steel Structures, St. Louis, Missouri, U.S.A.

CSA (1994), Cold Formed Steel Structural Members, A National Standard of Canada, Canadian Standards Association, Rexdale, Ontario, Canada.

Ingvarsson, L. (1977), Cold-Forming Residual Stresses in Thin-Walled Structures, International Conference on Thin-Walled Structures, Glasgow, Scotland.

Kanok-Nukulchai, W. (1990), Development of a Powerful Nonlinear Analysis Package for Small Computers, International Conference on Education, Practice, and Promotion of Computational Methods in Engineering using Small Computers, Macau.

Karren, K. W. (1967), Corner Properties of Cold-Formed Steel Shapes, Journal of the Structural Division, ASCE Proceedings, Vol. 93, No. ST1, pp. 401-432.

Karren, K. W. and Winter, G. (1967), Effects of Cold-Forming on Light-Gage Steel Members, Journal of the Structural Division, ASCE Proceedings, Vol. 93, No. ST1, pp. 433-469.

Weller, E. J. and Haavisto, M. (1984), Nontraditional Machining Processes, Society of Manufacturing Engineers, Dearborn, Michigan, U.S.A.

Weng, C. C. and Pekoz, T. (1990), Residual Stresses in Cold-Formed Steel Members, Journal of Structural Engineering, ASCE, Vol. 116, No. 6, pp. 1611-1625.

Appendix: Notations

E	Modulus of elasticity of material.	F_{yc}	Yield strength of corner zone material.
E_T	Tangent modulus of material.	ΔF_y	Increase in yield strength of corner zone.
F_p	Proportional limit.	P_u	Ultimate load of section
F_{rl}	Longitudinal residual stress.	r	Inside bending radius of corner.
F_u	Ultimate strength of material.	t	Thickness of steel sheet.
F_y	Yield strength of flat zone material.		

EVALUATION AND MODELLING OF THE MATERIAL PROPERTIES FOR ANALYSIS OF COLD-FORMED STEEL SECTIONS

Nabil Abdel-Rahman and K. S. Sivakumaran

Executive Summary

The results of two series of experimental investigations on cold-formed steel (CFS) channel sections are reported. Tensile coupon tests were used to evaluate the mechanical properties and strain gauges with an "Electrical Discharge Machining" technique were used to establish the distributions of residual stresses. Mechanical properties and residual stress distributions are idealized based on the experimental results. The idealizations are incorporated within a finite element model for CFS sections, and the model is evaluated against experiments of sections in compression.